ENDOSCOPE EFFECTS ON MHD PERISTALTIC FLOW OF A POWER-LAW FLUID

T. HAYAT, E. MOMONIAT, AND F. M. MAHOMED

Received 27 January 2005; Revised 5 October 2005; Accepted 8 November 2005

To understand the influence of an inserted endoscope and magnetohydrodynamic (MHD) power-law fluid on peristaltic motion, an attempt has been made for flow through tubes. The magnetic field of uniform strength is applied in the transverse direction to the flow. The analysis has been performed under long wavelength at low-Reynolds number assumption. The velocity fields and axial pressure gradient have been evaluated analytically. Numerical results are also presented and discussed.

1. Introduction

In the functioning of ureters, intestines, esophagus, and in medical instruments such as the heart-lung machine, fluid is transported by a unique process; a series of contractions of the wall propagates along the length of the tube causing fluid to be transported in the direction of the wave. This is called peristaltic pumping. The problem of peristaltic transport in two-dimensional channels and in axisymmetric tubes has received considerable attentioin. Several investigators [2, 3, 6, 9, 13, 14, 20, 24, 26, 28, 31–33, 35, 36, 38, 39] reported the studies of peristaltic hydrodynamic flows of Newtonian and non-Newtonian fluids.

Biomagnetic fluid dynamics is a relatively new area that deals with the fluid dynamics of magnetohydrodynamic biological fluids. During the last decades, extensive literature is available on the MHD flows of biological fluids. Such flows have numerous applications in bioengineering and medical sciences. Specifically, magnetic wound or cancer tumor treatment causing magnetic hyperthermia, bleeding reduction during surgeries, and targeted transport of drugs using magnetic particles as drug carriers are few such examples. In fact, a biomegnetic fluid exists in a living creature and its flow is effected through a magnetic field. Blood is a biomagnetic fluid. It behaves as a magnetic fluid, due to the complex interaction of the intercellular protein, cell membrane, and the hemoglobin. It is also known that blood possesses the property of diamagnetic material when oxygenated

Hindawi Publishing Corporation
Mathematical Problems in Engineering
Volume 2006, Article ID 84276, Pages 1–19
DOI 10.1155/MPE/2006/84276

and paramagnetic when deoxygenated. Only few studies [1, 37, 40] deal with the peristaltic transport of magnetohydrodynamic flows. In the studies [19, 23, 30], the blood is effected by a magnetic field under physiological conditions. More recently, Misery et al. [21] and Hakeem et al. [8] discussed the effects of an endoscope on the peristaltic motion involving hydrodynamic Newtonian and generalized Newtonian fluids, respectively. To make the mathematical problem tractable, the above-mentioned studies are examined under one or more simplifying assumptions. Note that the endoscopes are either semirigid or completely rigid tubes that can only be inserted with the exertion of considerable force by a physician. As a consequence, they are liable to damage the internal vessels of the body and may induce patient discomfort during insertion. Even catheters, which are more flexible, can do damage when pushed into the different vessels and lumens of the body [4, 5, 7, 41]. Recently, there have been several attempts to use biological inspiration as the basis for novel endoscopes. Keeping in view the flexible movements of snakes, Hirose [12] has studied the endoscopes that can bend in response to the activation of shape memory alloy wires.

It is the purpose of the present investigation to see the effects of an endoscope on the magnetohydrodynamic flow of a power-law fluid. It is a well-accepted fact that blood, in a homogenized sense, can be modeled as a power-law fluid while flowing in large blood vessels (see [15] and several references therein). Although the power-law model is known widely, yet it does not exhibit significant normal stress differences. The viscosity however depends strongly on the rate of shear. It is worth remarking that for shear-thinning fluids, the zero-shear rate viscosity blows up. In the case of a shear-thickening fluids, their generalized velocities tend to zero as the shear rate goes to zero. For detailed discussion of the various forms of generalized viscosities, we refer the reader to the paper by Málek et al. [17]. This study deals with issues concerning mathematical results, especially concerning the existence, uniqueness, and stability of flows of fluids that can shear-thicken or shear-thin. A discussion on issues concerning non-Newtonian fluids, the behavior of various types of power-law fluids, and more general fluids of complexity one can be found in the survey article by Rajagopal [25]. The results concerning the stability and uniqueness of flows of fluids of complexity n, and hence complexity one, are described in great length. Moreover, rigorous mathematical results have been established for fluid that can shear-thin or shear-thicken in the book of Málek et al. [16]. The reader may consult this book for relevant details of definitions of weak solution, derivation of several inequalities, the limiting processes, and so forth.

From fluid dynamics point of view, there is no difference between an endoscope and catheter, but from physiological point of view we cannot use a catheter for small intestine. The assumption for the present analysis is that the wavelength of the peristaltic wave is large compared with the radius of the outer tube. This assumption is similar to those used in the references [10, 11, 18, 22, 27, 29, 30, 32, 34, 36]. The solution to the governing nonlinear problem is given. The results for pressure rise and frictional forces on the inner and outer tubes have been computed numerically. Comparison is made between the results for hydrodynamic fluid and the magnetohydrodynamic fluid. The difference between the results of Newtonian and power-law fluid is noted. Finally, the results of an endoscope on the flow are also discussed.

2. Position of the problem

We consider the MHD flow of a power-law fluid through coaxial uniform tubes. The inner tube is rigid while the outer tube has a sinusoidal wave travelling down its wall. We choose cylindrical coordinates $(\overline{R},\overline{Z})$ such that $\overline{Z}$-axis is along the centerline of the inner and outer tubes and $\overline{R}$ is the distance measured radially. The conducting fluid is permeated by an imposed uniform magnetic field $\mathbf{B}_0$ which acts in the transverse direction. In the low-magnetic-Reynolds number case, in which the induced magnetic field can be ignored, the magnetic body force $\mathbf{J}\times\mathbf{B}_0$ becomes $\sigma(\mathbf{V}\times\mathbf{B}_0)\times\mathbf{B}_0$ when imposed, induced electric fields are negligible, and only the magnetic field $\mathbf{B}_0$ contributes to the current $\mathbf{J}=\sigma(\mathbf{V}\times\mathbf{B}_0)$. Here, $\mathbf{V}$ is the velocity and σ is the electrical conductivity of the fluid, which has density ρ and dynamic viscosity μ.

The motion of an incompressible MHD flow is described through the following equations:

$$\begin{aligned}
\rho\left[\frac{\partial}{\partial\overline{t}}+\overline{U}\frac{\partial}{\partial\overline{R}}+\overline{W}\frac{\partial}{\partial\overline{Z}}\right]\overline{U} &= -\frac{\partial\overline{p}}{\partial\overline{R}}+\frac{1}{\overline{R}}(\overline{R}\overline{S}_{\overline{R}\overline{R}})+\frac{\partial}{\partial\overline{Z}}(\overline{S}_{\overline{R}\overline{Z}})-\frac{\overline{S}_{\overline{\theta}\overline{\theta}}}{\overline{R}},\\
\rho\left[\frac{\partial}{\partial\overline{t}}+\overline{U}\frac{\partial}{\partial\overline{R}}+\overline{W}\frac{\partial}{\partial\overline{Z}}\right]\overline{W} &= -\frac{\partial\overline{p}}{\partial\overline{Z}}+\frac{1}{\overline{R}}\frac{\partial}{\partial\overline{R}}(\overline{R}\overline{S}_{\overline{R}\overline{Z}})+\frac{\partial}{\partial\overline{Z}}(\overline{S}_{\overline{Z}\overline{Z}})-\sigma B_0^2\overline{W},\\
\frac{1}{\overline{R}}\frac{\partial}{\partial\overline{R}}(\overline{R}\overline{U})+\frac{\partial\overline{W}}{\partial\overline{Z}} &= 0.
\end{aligned}\tag{2.1}$$

In the above equations, $\overline{t}$ is the time, $\overline{p}$ is the pressure, $\overline{U}$ and $\overline{W}$ are radial and axial velocities, respectively, in the fixed frame, and for a power-law fluid, the extra-stress tensor $\overline{\mathbf{S}}$ is [12]

$$\overline{\mathbf{S}}=\mu\left[\operatorname{tr}\left(\overline{\mathbf{A}}_1^2\right)\right]^m\overline{\mathbf{A}}_1,\tag{2.2}$$

where tr is the trace, m is the power-law exponent, and the first kinematical tensor $\overline{\mathbf{A}}_1$ is

$$\overline{\mathbf{A}}_1=\left(\overline{\nabla\mathbf{V}}\right)+\left(\overline{\nabla\mathbf{V}}\right)^*,\tag{2.3}$$

in which $(*)$ is the matrix transpose. It should be noted that for $m=0$, we get the results for Newtonian fluids, while for $m<0$ $(m>0)$ corresponds to the results of shear-thinning (shear-thickening) fluids.

The geometries of the wall surfaces are

$$\overline{r}_1=a_1,\tag{2.4}$$

$$\overline{r}_2=a_2+b\sin\frac{2\pi}{\lambda}(\overline{Z}-c\overline{t}),\tag{2.5}$$

where a_1 is the radius of the inner tube, a_2 is the radius of the outer tube at the inlet, c is the wave speed, b is the wave amplitude, and λ is the wavelength.

In the fixed coordinate system $(\overline{R},\overline{Z})$, the motion is unsteady because of the moving boundary. However, if observed in a coordinate system $(\overline{r},\overline{z})$ moving at the speed c, it can

be treated as steady because the boundary shape appears to be stationary. The relationship between the two coordinate frames is given by

$$\begin{aligned} \overline{z} &= \overline{Z} - c\overline{t}, \qquad \overline{r} = \overline{R}, \\ \overline{w}(\overline{r},\overline{z}) &= \overline{W}(\overline{R},\overline{Z}-c\overline{t}) - c, \qquad \overline{u}(\overline{r},\overline{z}) = \overline{U}(\overline{R},\overline{Z}-c\overline{t}), \end{aligned} \tag{2.6}$$

in which $\overline{u}$ and $\overline{w}$ are the radial and axial velocities in the moving frame.

The boundary conditions in the moving frame are

$$\overline{w} = -c \quad \text{at } \overline{r} = \overline{r}_1,\ \overline{r} = \overline{r}_2, \qquad \overline{u} = 0 \quad \text{at } \overline{r} = \overline{r}_1. \tag{2.7}$$

Using relationship (2.6) introducing the following nondimensional variables and parameters

$$\begin{aligned} \overline{r} &= a_2 r, \qquad \overline{z} = \lambda z, \qquad \overline{u} = \frac{a_2 c u}{\lambda}, \\ r_1 &= \frac{\overline{r}_1}{a_2} = \frac{a_1}{a_2} = \epsilon < 1, \qquad \overline{w} = cw, \\ r_2 &= \frac{\overline{r}_2}{a_2} = 1 + \phi \sin(2\pi z), \qquad \mathbf{S} = \frac{\mu c}{a_2}\left(\frac{2c^2}{a_2^2}\right)^m \overline{\mathbf{S}}, \\ \overline{p} &= \frac{c\lambda\mu}{a_2^2} p\left(\frac{2c^2}{a_2^2}\right)^m, \qquad \delta = \frac{a_2}{\lambda}, \qquad \phi = b/a_2 (< 1), \\ \mathrm{Re} &= \frac{\rho c a_2}{\mu}\left(\frac{a_2^2}{2c^2}\right)^m, \qquad M^2 = \frac{\sigma B_0^2}{\mu} a_2^2 \left(\frac{a_2^2}{2c^2}\right)^m, \end{aligned} \tag{2.8}$$

(2.1) and boundary conditions (2.7) become

$$\mathrm{Re}\ \delta^3 \left[u\frac{\partial}{\partial r} + w\frac{\partial}{\partial z}\right]u = -\frac{\partial p}{\partial r} + \delta\left[\frac{1}{r}\frac{\partial}{\partial r}(rS_{rr}) + \delta\frac{\partial}{\partial z}S_{rz} - \frac{S_{\theta\theta}}{r}\right], \tag{2.9}$$

$$\mathrm{Re}\,\delta\left[u\frac{\partial}{\partial r} + w\frac{\partial}{\partial z}\right]w = -\frac{\partial p}{\partial z} + \left[\frac{1}{r}\frac{\partial}{\partial r}(rS_{rz}) + \delta\frac{\partial}{\partial z}S_{zz}\right] - M^2(w+1), \tag{2.10}$$

$$\frac{1}{r}\frac{\partial}{\partial r}(ru) + \frac{\partial w}{\partial z} = 0, \tag{2.11}$$

$$w = -1 \quad \text{at } r = r_1 = \epsilon,\ r = r_2 = 1 + \phi \sin 2\pi z, \tag{2.12}$$

$$u = 0 \quad \text{at } r = r_1. \tag{2.13}$$

In the above equations, δ is the wave number, ϕ is the amplitude ratio, Re is the generalized Reynolds number, M is the generalized Hartmann number, and

$$S_{rr} = 2\delta\left[2\delta^2\left(\frac{\partial u}{\partial r}\right)^2 + \left(\frac{\partial w}{\partial r} + \delta^2\frac{\partial u}{\partial z}\right)^2 + 2\delta^2\left(\frac{u}{r}\right)^2 + 2\delta^2\left(\frac{\partial w}{\partial z}\right)^2\right]^m \frac{\partial u}{\partial r}, \tag{2.14}$$

$$S_{rz} = \left[2\delta^2\left(\frac{\partial u}{\partial r}\right)^2 + \left(\frac{\partial w}{\partial r} + \delta^2\frac{\partial u}{\partial z}\right)^2 + 2\delta^2\left(\frac{u}{r}\right)^2 + 2\delta^2\left(\frac{\partial w}{\partial z}\right)^2\right]^m \left(\frac{\partial w}{\partial r} + \delta^2\frac{\partial u}{\partial z}\right), \tag{2.15}$$

$$S_{\theta\theta} = 2\delta\left[2\delta^2\left(\frac{\partial u}{\partial r}\right)^2 + \left(\frac{\partial w}{\partial r} + \delta^2\frac{\partial u}{\partial z}\right)^2 + 2\delta^2\left(\frac{u}{r}\right)^2 + 2\delta^2\left(\frac{\partial w}{\partial z}\right)^2\right]^m \frac{u}{r}, \tag{2.16}$$

$$S_{zz} = 2\delta\left[2\delta^2\left(\frac{\partial u}{\partial r}\right)^2 + \left(\frac{\partial w}{\partial r} + \delta^2\frac{\partial u}{\partial z}\right)^2 + 2\delta^2\left(\frac{u}{r}\right)^2 + 2\delta^2\left(\frac{\partial w}{\partial z}\right)^2\right]^m \frac{\partial w}{\partial z}. \tag{2.17}$$

For long-wavelength analysis, (2.9), (2.10), and (2.14)–(2.17) give

$$-\frac{\partial p}{\partial r} = 0, \tag{2.18}$$

$$\frac{\partial p}{\partial z} = \frac{1}{r}\frac{\partial}{\partial r}\left[r\left(\frac{\partial w}{\partial r}\right)^{2m+1}\right] - M^2(w+1). \tag{2.19}$$

Equation (2.18) indicates that p is not a function of r. Hence, p is only a function of z.

The expressions for flow rate (F), pressure rise (ΔP_λ) and frictional forces on inner ($F_\lambda^{(i)}$) and outer ($F_\lambda^{(0)}$) tubes in nondimensional variables are [19, 21]

$$F = \int_{r_1}^{r_z} wr\,dr, \tag{2.20}$$

$$\Delta P_\lambda = \int_0^1 \left(\frac{dp}{dz}\right)dz, \tag{2.21}$$

$$F_\lambda^{(i)} = \int_0^1 r_1^2\left(-\frac{dp}{dz}\right)dz, \tag{2.22}$$

$$F_\lambda^{(0)} = \int_0^1 r_2^2\left(-\frac{dp}{dz}\right)dz. \tag{2.23}$$

3. Analytical and numerical solutions

In this section, we consider analytical solutions for the case, $m = 0$. For this particular case we are able to determine the pressure gradient dp/dz in terms of the flow rate F. We use this result for dp/dz in the numerical solution for the case $m \neq 0$. This allows us to determine the effect of m on the fluid velocities. Choosing $m = 0$, (2.19) reduces to

$$\frac{\partial^2 w}{\partial r^2} + \frac{1}{r}\frac{\partial w}{\partial r} - M^2(w+1) - G(z) = 0, \tag{3.1}$$

where $G(z) = dp/dz$. Solving (3.1) subject to the boundary conditions (2.12), we obtain

$$\begin{aligned} w(r,z) = {} & \left[M^2\left(-\left(I_0(Mr_2(z))K_0(\epsilon M)\right) + I_0(\epsilon M)K_0\left(Mr_2(z)\right)\right)\right]^{-1} \\ & \times \left\{M^2\left(I_0(Mr_2(z))K_0(\text{eps } M) - I_0(\epsilon M)K_0\left(Mr_2(z)\right)\right)\right. \\ & + \left(\left(-I_0(Mr) + I_0\left(Mr_2(z)\right)\right)K_0(\epsilon M)\right. \\ & + \left(I_0(\epsilon M) - I_0\left(Mr_2(z)\right)\right)K_0(Mr) \\ & \left.\left. + \left(-I_0(\epsilon M) + I_0(Mr)\right)K_0\left(Mr_2(z)\right)\right)G(z)\right\}, \end{aligned} \tag{3.2}$$

where I_0 is the modified Bessel function of the first kind of order 0, K_0 is the modified Bessel function of the second kind of order 0. Substituting (3.2) into (2.11) and solving subject to (2.13), we find that

$$\begin{aligned}
u(r,z) = &\left[2M^4 r\left(I_0(Mr_2(z))K_0(\epsilon M) - I_0(\epsilon M)K_0(Mr_2(z))\right)^2 r_2(z)\right]^{-1} \\
&\times \left(I_0(Mr_2(z))K_0(\epsilon M) - I_0(\epsilon M)K_0(Mr_2(z))\right) \\
&\times \left(2 + M\left(M\left(-\left(r^2 I_0(\epsilon M)\right) + \epsilon^2 I_2(\epsilon M)\right)K_0(Mr_2(z))\right.\right. \\
&\quad + 2rI_1(Mr)\left(-K_0(\epsilon M) + K_0(Mr_2(z))\right) - 2rI_0(\epsilon M)K_1(Mr) \\
&\quad \left.\left. + I_0(Mr_2(z))\left(Mr^2 K_0(\epsilon M) + 2rK_1(Mr) - \epsilon^2 MK_2(\epsilon M)\right)\right)r_2(z)G'(z)\right. \\
&\quad + 2\left(-1 + MrI_1(Mr)K_0(\epsilon M)\right. \\
&\qquad \left. + MrI_0(\epsilon M)K_1(Mr)\right)G(z)\left(-1 + M\left(I_1(Mr_2(z))K_0(\epsilon M)\right.\right. \\
&\qquad \left.\left. + I_0(\epsilon M)K_1(Mr_2(z))\right)r_2(z)\right)r_2{}'(z).
\end{aligned} \tag{3.3}$$

We can determine the pressure gradient in terms of the flow rate by substituting (3.2) into (2.20) and solving for $G(z)$. We find that

$$\begin{aligned}
G(z) = \frac{dp}{dz} = &\left[4 + \epsilon^2 M^2\left(I_2(\epsilon M)K_0(Mr_2(z)) - I_0(Mr_2(z))K_2(\epsilon M)\right)\right. \\
&\quad + Mr_2(z)\left(-2\left(I_1(Mr_2(z))K_0(\epsilon M) + I_0(\epsilon M)K_1(Mr_2(z))\right)\right. \\
&\quad \left.\left. + M\left(I_0(Mr_2(z))K_0(\epsilon M) - I_0(\epsilon M)K_0(Mr_2(z))\right)r_2(z)\right)\right]^{-1} \\
&\times \left\{M^4\left(I_0(Mr_2(z))K_0(\epsilon M) - I_0(0,\epsilon M)K_0(Mr_2(z))\right)\left(\epsilon^2 - 2F - r_2(z)^2\right)\right\}.
\end{aligned} \tag{3.4}$$

When we take both $m = 0$ and $M = 0$, then (2.19) reduces to

$$\frac{\partial^2 w}{\partial r^2} + \frac{1}{r}\frac{\partial w}{\partial r} - G(z) = 0. \tag{3.5}$$

We determine the velocity components and pressure gradient in the same way as indicated above and get

$$\begin{aligned}
w(r,z) = &\left[4\left(\log(\epsilon) - \log\left(r_2(z)\right)\right)\right]^{-1} \\
&\times \left\{-4\log(\epsilon) + 4\log\left(r_2(z)\right)\right. \\
&\quad + G(z)\left(r^2\log(\epsilon) - \epsilon^2\log(r) + \epsilon^2\log\left(r_2(z)\right)\right. \\
&\qquad \left.\left. - r^2\log\left(r_2(z)\right) + \left(-\log(\epsilon) + \log(r)\right)r_2(z)^2\right)\right\},
\end{aligned} \tag{3.6}$$

$$
\begin{aligned}
u(r,z) = {} & \left[16r\left(\log(\epsilon)-\log\left(r_2(z)\right)\right)^2 r_2(z)\right]^{-1} \\
& \times \left\{\left(\log(\epsilon)-\log\left(r_2(z)\right)\right) r_2(z) \right. \\
& \quad \times \left(\left(-\epsilon^4-r^4\right)\log(\epsilon)\right. \\
& \qquad + \epsilon^2\left(\epsilon^2-r^2+2r^2\log(r)\right)+\left(\epsilon^2-r^2\right)^2\log\left(r_2(z)\right) \\
& \qquad \left. + \left(-\epsilon^2+r^2+2r^2\left(\log(\epsilon)-\log(r)\right)\right) r_2(z)^2\right) G'(z) \\
& \quad + G(z)\left((\epsilon-r)(\epsilon+r)+2r^2\left(-\log(\epsilon)+\log(r)\right)\right) \\
& \quad \left. \times \left(\epsilon^2+\left(-1-2\log(\epsilon)+2\log\left(r_2(z)\right)\right) r_2(z)^2\right) r_2'(z)\right\},
\end{aligned}
\tag{3.7}
$$

$$
\begin{aligned}
G(z) = \frac{dp}{dz} = {} & \left[\epsilon^4\left(-1+\log(\epsilon)-\log\left(r_2(z)\right)\right)\right. \\
& \left. + 2\epsilon^2 r_2(z)^2+\left(-1-\log(\epsilon)+\log\left(r_2(z)\right)\right) r_2(z)^4\right]^{-1} \\
& \times \left\{-8\left(\log(\epsilon)-\log\left(r_2(z)\right)\right)\left(\epsilon^2-2F-r_2(z)^2\right)\right\}.
\end{aligned}
\tag{3.8}
$$

For the case $m \neq 0$, we try to solve (3.1) subject to the boundary conditions (2.12) numerically. The partial differential equation (3.1) can be written as

$$
\frac{\partial^2 w}{\partial r^2} = \frac{M^2 r + rG(z) + M^2 rw - (\partial w/\partial r)^{2m+1}}{(2m+1)r(\partial w/\partial r)^{2m}}. \tag{3.9}
$$

When $m = 0$ the denominator of (3.9) is just r. Since the domain of the problem is $r \in [\epsilon, r_2(z)]$, this does not present a problem when solving (3.9) for the case $m = 0$ subject to (2.12). For $m \neq 0$ as

$$
\left(\frac{\partial w}{\partial r}\right)^{2m} \longrightarrow 0, \tag{3.10}
$$

the partial differential equation becomes singular. As m increases, (3.9) becomes singular much faster. This singular nature of the partial differential equation makes it difficult to fit the boundary conditions (2.12) when trying to determine a numerical solution of (2.19) for arbitrary m.

Instead, we consider an approximate solution of the form

$$
w = w_0 + mw_1, \quad m \ll 1. \tag{3.11}
$$

Substituting (3.11) into (2.19), taking $dp/dz = G(z)$, and separating to leading order in m, we obtain (3.2) and

$$
\frac{\partial^2 w_1}{\partial r^2} + \frac{1}{r}\frac{\partial w_1}{\partial r} - M^2 w_1 + 2\frac{\partial^2 w_0}{\partial r^2}\left(1+\log\left(\frac{\partial w_0}{\partial r}\right)\right) + \frac{2}{r}\frac{\partial w_0}{\partial r}\log\left(\frac{\partial w_0}{\partial r}\right) = 0. \tag{3.12}
$$

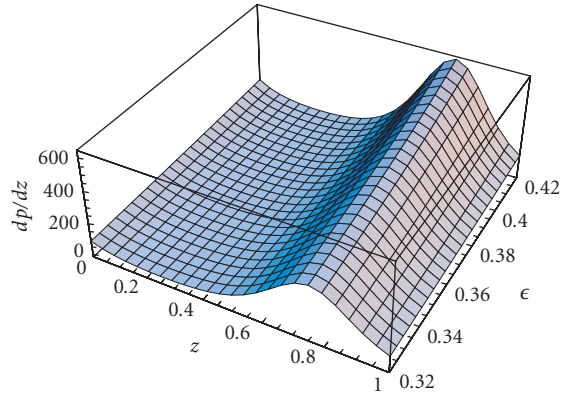

(a)

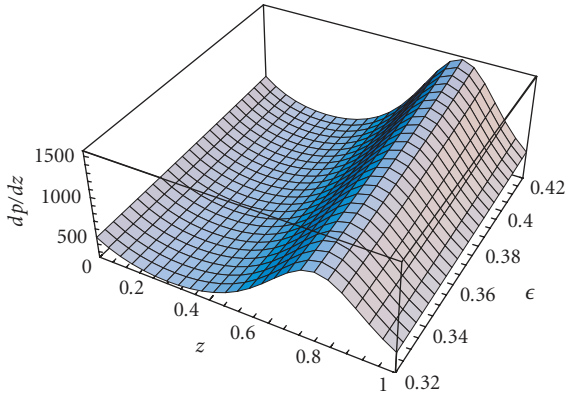

(b)

Figure 4.1. Plot showing the effects of changing ϵ on the pressure gradient dp/dz for (a) $M = 0$ (b) $M = 10$.

Equation (3.12) is solved numerically subject to the boundary conditions

$$w_1(\epsilon) = 0, \qquad w_1(r_2(z)) = 0. \tag{3.13}$$

When solving (3.12) numerically for the case $M \neq 0$, $G(z)$ is given by (3.4) and w_0 is given by (3.2). For the case $M = 0$, $G(z)$ is given by (3.8) and w_0 is given by (3.6).

4. Discussion

In Figures 4.1, 4.2, and 4.3, we plot the effect of changing ϵ, flow rate, and amplitude ratio ϕ on the pressure gradient dp/dz for generalized Hartmann numbers $M = 0$ and

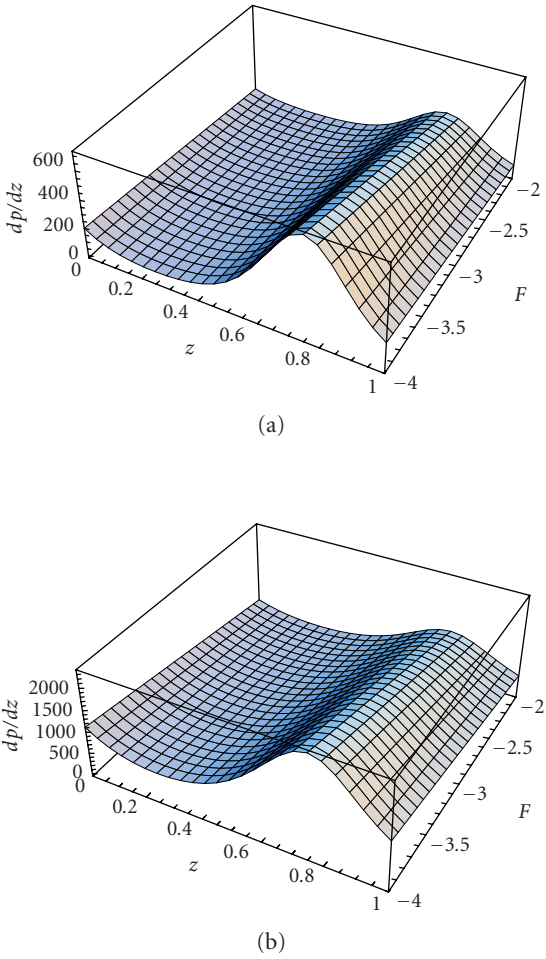

Figure 4.2. Plot showing the effects of changing flow rate F on the pressure gradient dp/dz for (a) $M = 0$ (b) $M = 10$.

$M = 10$. We observe that the pressure gradient increases with increasing ϵ, flow rate F, and amplitude ratio ϕ. The increase in generalized Hartmann number also causes an increase in the pressure gradient.

The effects of changing ϵ, flow rate and amplitude ratio ϕ on the pressure rise ΔP_λ, inner frictional force $F_\lambda^{(i)}$ and outer frictional force $F_\lambda^{(o)}$ are plotted in Figures 4.4, 4.5 and 4.6. Here we observe that increasing generalized Hartmann number increases the magnitude of the pressure rise, inner, and outer frictional forces. The pressure rise increases and the frictional forces decrease with the increase in the values of ϵ, flow rate, and amplitude ratio.

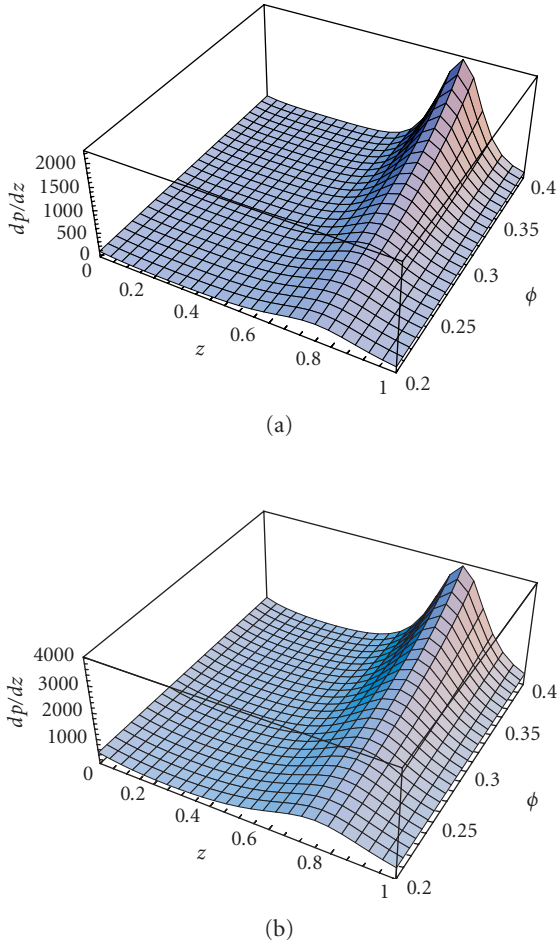

Figure 4.3. Plot showing the effects of changing amplitude ratio ϕ on the pressure gradient dp/dz for (a) $M = 0$ (b) $M = 10$.

The effects of increasing generalized Hartmann number on the velocities w and u are plotted in Figure 4.7. We note that the increase in generalized Hartmann number reduces the magnitude of the velocity w while increasing the velocity of u. In both cases, the nonlinearity of the velocity profiles is amplified by increasing generalized Hartmann number.

In Figure 4.8, we plot the numerical solution of (3.12) for $M = 0$ and $M = 10$. We note that increasing the generalized Hartmann number reduces the amplitude of w_1. The velocity $w = w_0 + mw_1$ is plotted in Figure 4.9 for $M = 0$ and $M = 5$. We observe that in both cases $M = 0$ and $M = 5$, increasing m causes a decrease in the magnitude of the velocity. In Figure 4.10 we plot the numerical solution of (2.11) subject to (2.13), where we have taken $w = w_0 + mw_1$ and evaluated the derivative $\partial w/\partial z$ using a forward-difference

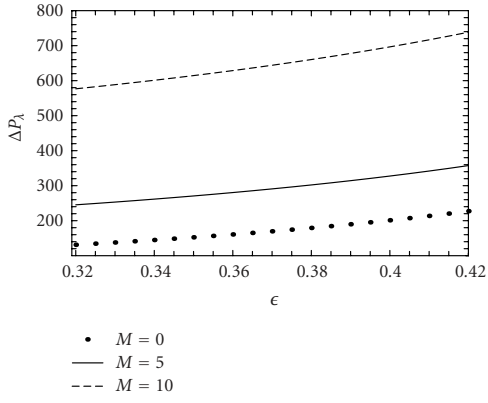

(a)

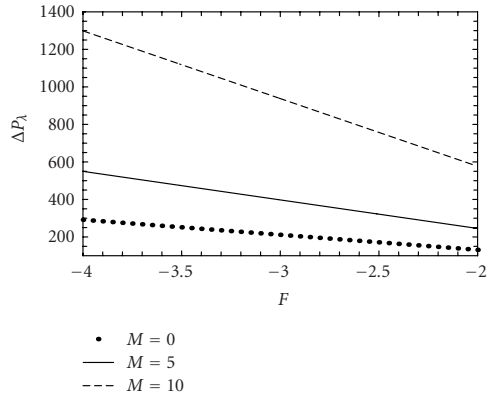

(b)

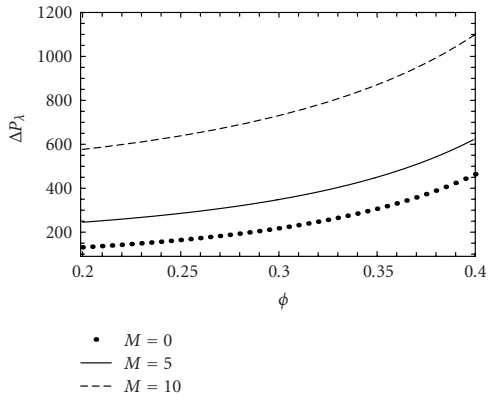

(c)

Figure 4.4. Plot of the pressure rise Δp_λ showing the effects of changing ϵ, flow rate F, and amplitude ratio ϕ for $M = 0$, $M = 5$, and $M = 10$. (a) $F = -2$, $\phi = 0.2$, (b) $\epsilon = 0.32$, $\phi = 0.2$, and (c) $F = -2$, $\epsilon = 0.32$.

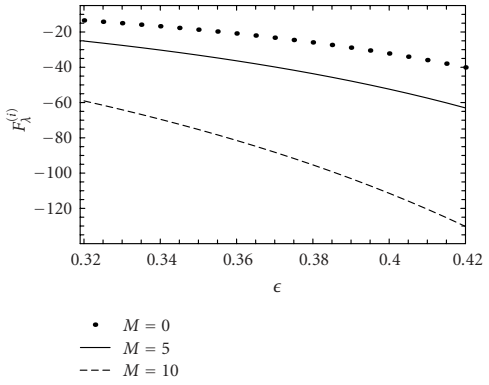

(a)

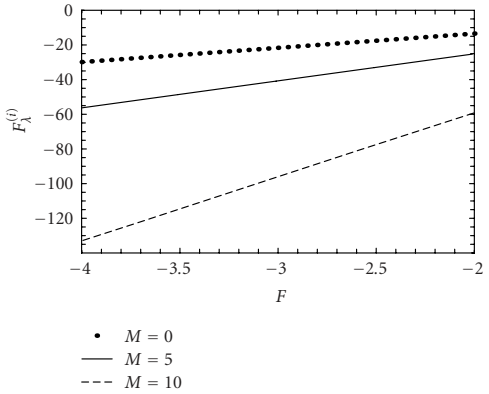

(b)

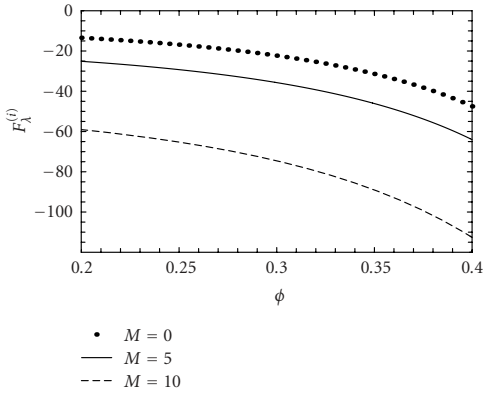

(c)

Figure 4.5. Plot of the frictional force on the inner tube $F_\lambda^{(i)}$ showing the effects of changing ϵ, flow rate F, and amplitude ratio ϕ for $M = 0$, $M = 5$, and $M = 10$. (a) $F = -2$, $\phi = 0.2$, (b) $\epsilon = 0.32$, $\phi = 0.2$, and (c) $F = -2$, $\epsilon = 0.32$.

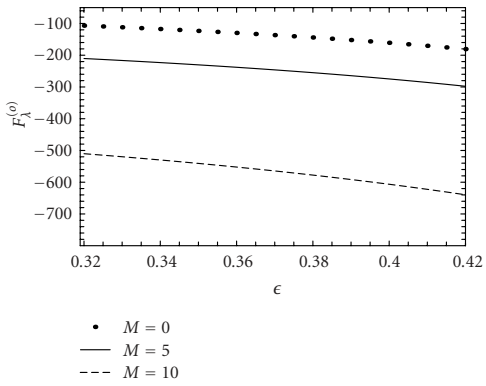

(a)

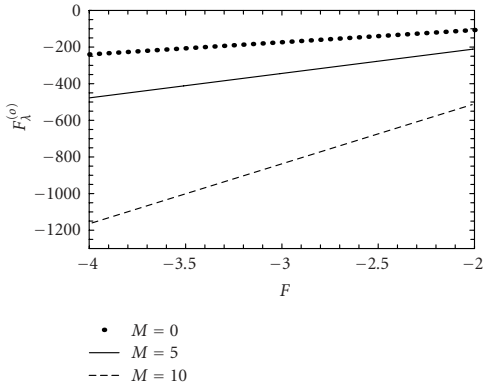

(b)

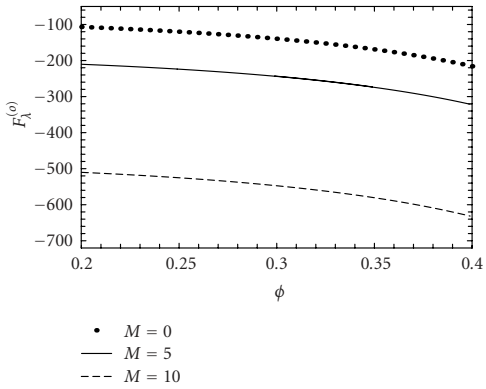

(c)

Figure 4.6. Plot of the frictional force on the outer tube $F_\lambda^{(o)}$ showing the effects of changing ϵ, flow rate F, and amplitude ratio ϕ for $M = 0$, $M = 5$, and $M = 10$. (a) $F = -2$, $\phi = 0.2$, (b) $\epsilon = 0.32$, $\phi = 0.2$, and (c) $F = -2$, $\epsilon = 0.32$.

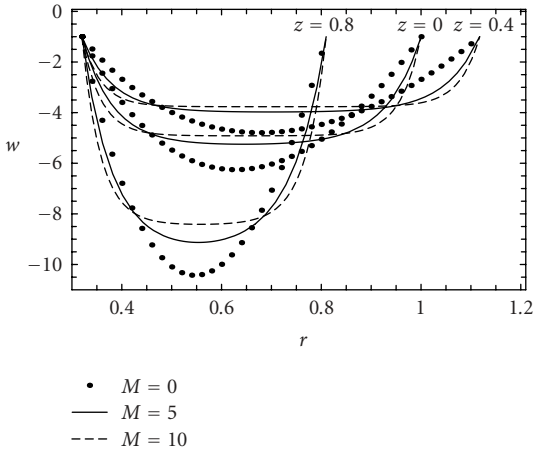

(a)

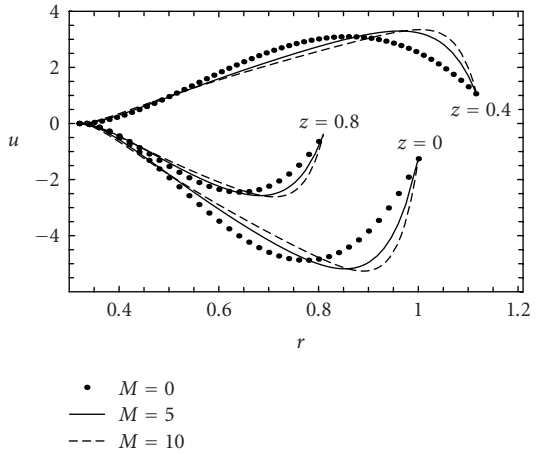

(b)

Figure 4.7. Plot of the velocities $w(r,z)$ and $u(r,z)$ for $M = 0$, $M = 5$, and $M = 10$, where $F = -2$, $\phi = 0.2$, and $\epsilon = 0.32$.

scheme $w(r,z+h) - w(r,z)/h$ taking $h = 0.001$. We observe that increasing m reduces the magnitude of the velocity.

5. Concluding remarks

In this paper, peristaltic flow of an incompressible power-law fluid has been studied in the presence of magnetic field. The effects of an endoscope on the flow have been shown.

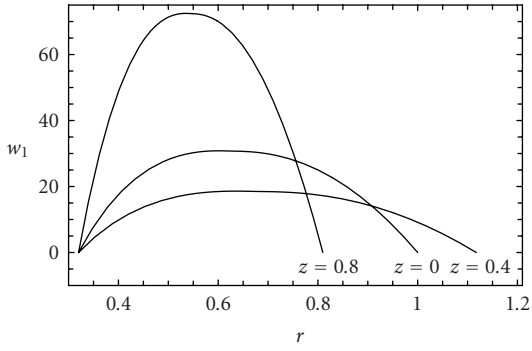

(a)

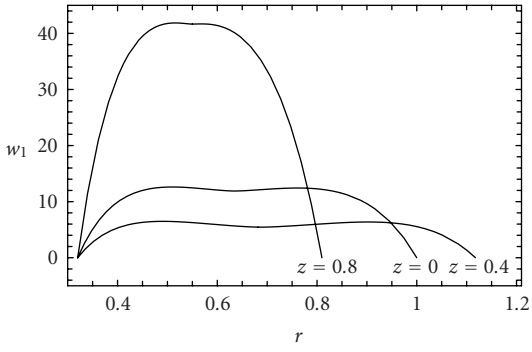

(b)

Figure 4.8. Plot of the numerical solution of $w_1(r,z)$ for (a) $M = 0$ and (b) $M = 5$, where $F = -2$, $\phi = 0.2$, and $\epsilon = 0.32$.

The governing nonlinear equation is solved to examine the dependence of the flow on the power-law exponent in the constitutive model, the applied magnetic field, the flow rate, the amplitude ratio, and the radius ratio. The comparison between the results of Newtonian and power-law model has been made. The following conclusions have been found and summarized as follows.

(a) With the increase of flow rate, amplitude ratio, and radius ratio, the pressure gradient increases.

(b) The pressure gradient may be increased by increasing generalized Hartmann number.

(c) The magnitude of velocity may be decreased with increment in power-law exponent.

(d) The pressure rise increases with increasing radius ratio, flow rate, and amplitude ratio. The behavior of the frictional forces is opposite to that of the pressure rise.

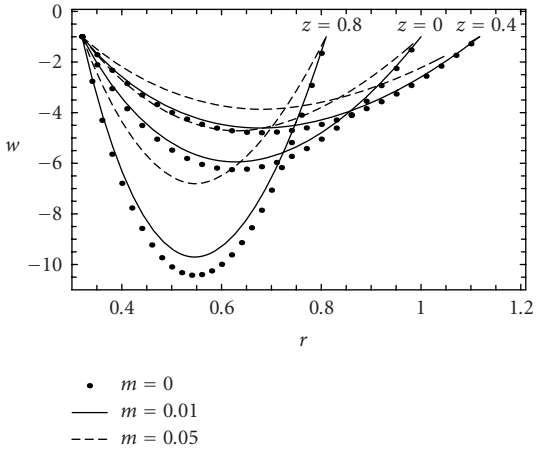

(a)

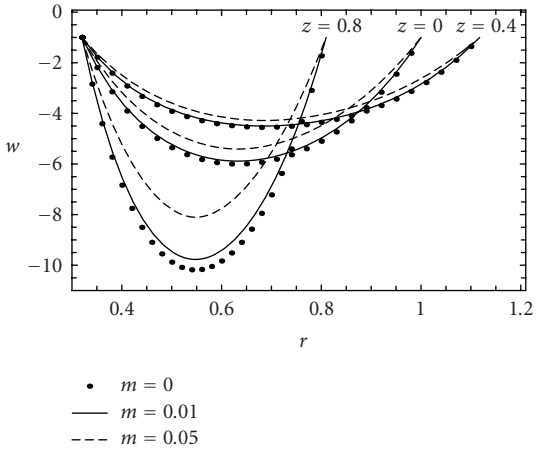

(b)

Figure 4.9. Plot of the velocity $w = w_0 + mw_1$ for (a) $M = 0$, (b) $M = 5$, where $m = 0$, $m = 0.01$, $m = 0.05$, $F = -2$, $\phi = 0.2$, and $\epsilon = 0.32$.

(e) The increment in the generalized Hartmann number produces large values of u and small values of w.

(f) The present study seems to be the first attempt in the literature which deals the MHD non-Newtonian peristaltic flow along with an endoscope. Even, such attempt is not available in the literature for Newtonian fluid. Further aspects and developments on the problem can be investigated.

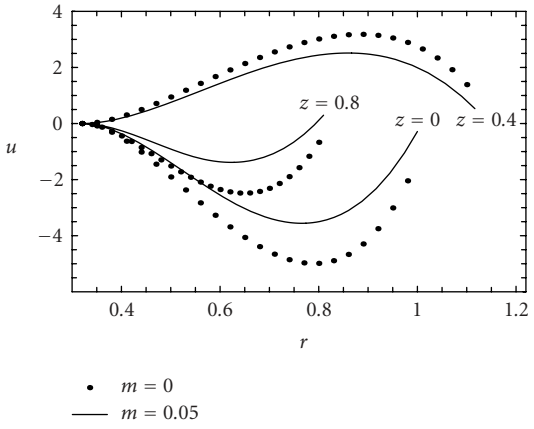

Figure 4.10. Plot of the velocity u for $M = 5$, where $m = 0$, $m = 0.05$, $F = -2$, $\phi = 0.2$, and $\epsilon = 0.32$.

Acknowledgments

We thank the referee for valuable comments that have enhanced the presentation of the paper. T. Hayat thanks the Differential Equations, Continuum Mechanics and Applications (DECMA) Research Centre and the School of Computational and Applied Mathematics at the University of the Witwatersrand, Johannesburg, for financial support and hospitality. E. Momoniat acknowledges support received from the National Research Foundation under Grant no. 2053745.

References

[1] H. L. Agrawal and B. Anwaruddin, *Peristaltic flow of blood in a branch*, Ranchi University Mathematical Journal **15** (1984), 111–121 (1985).

[2] T. D. Brown and T. K. Hung, *Computational and experimental investigations of two-dimensional non-linear peristaltic flows*, Journal of Fluid Mechanics **83** (1977), 249–272.

[3] J. C. Burns and T. Parkes, *Peristaltic motion*, Journal of Fluid Mechanics **29** (1967), 731–743.

[4] J. W. Folk, T. P. Joye, T. A. Duck, and M. K. Bailey, *Epidural catheters: the long and winding road*, Southern Medical Journal **93** (2000), 732–733.

[5] B. Funaki, G. X. Zaleski, J. Lorenz, P. B. Menocci, A. N. Funaki, J. D. Rosenblum, C. Straus, and J. A. Leef, *Radiologic gastrostomy placement: pigtail-versus mushroom-retained catheters*, American Journal of Roentgenology **175** (2000), 375–379.

[6] Y. C. Fung and C. S. Yih, *Peristaltic transport*, Journal of Applied Mechanics **35** (1968), 669–675.

[7] J. R. Grove and W. C. Pevec, *Venous thrombosis related to peripherally inserted central catheters*, Journal of Vascular and Interventional Radiology **11** (2000), 837–840.

[8] A. E. Hakeem, A. E. Naby, and A. E. M. Misery, *Effects of an endoscope and generalized Newtonian fluid on peristaltic motion*, Applied Mathematics and Computation **128** (2002), no. 1, 19–35.

[9] T. Hayat, Y. Wang, K. Hutter, S. Asghar, and A. M. Siddiqui, *Peristaltic transport of an Oldroyd-B fluid in a planar channel*, Mathematical Problems in Engineering **2004** (2004), no. 4, 347–376.

[10] T. Hayat, Y. Wang, A. M. Siddiqui, and K. Hutter, *Peristaltic motion of a Johnson-Segalman fluid in a planar channel*, Mathematical Problems in Engineering **2003** (2003), no. 1-2, 1–23.

[11] T. Hayat, Y. Wang, A. M. Siddiqui, K. Hutter, and S. Asghar, *Peristaltic transport of a third-order fluid in a circular cylindrical tube*, Mathematical Models & Methods in Applied Sciences **12** (2002), no. 12, 1691–1706.

[12] S. Hirose, *Biologically Inspired Robots: Snake-Like Locomotors and Manipulators*, Oxford University Press, Oxford, 1993.

[13] M. Y. Jaffrin and A. H. Shapiro, *Peristaltic pumping*, Annual Review of Fluid Mechanics **3** (1971), 13–37.

[14] N. Liron, *On peristaltic flow and its efficiency*, Bulletin of Mathematical Biology **38** (1976), no. 6, 573–596.

[15] J. Málek, J. Nečas, and K. R. Rajagopal, *Global analysis of the flows of fluids with pressure-dependent viscosities*, Archive for Rational Mechanics and Analysis **165** (2002), no. 3, 243–269.

[16] J. Málek, J. Nečas, M. Rokyta, and M. Ruzicka, *Weak and Measure-Valued Solutions to Evolutionary PDEs*, Applied Mathematics and Mathematical Computation, vol. 13, Chapman & Hall, London, 1996.

[17] J. Málek, K. R. Rajagopal, and M. Ruzicka, *Existence and regularity of solutions and the stability of the rest state for fluids with shear dependent viscosity*, Mathematical Models & Methods in Applied Sciences **5** (1995), no. 6, 789–812.

[18] D. Mansutti, G. Pontrelli, and K. R. Rajagopal, *Steady flows of non-Newtonian fluids past a porous plate with suction or injection*, International Journal for Numerical Methods in Fluids **17** (1993), no. 11, 927–941.

[19] Kh. S. Mekheimer, *Peristaltic flow of blood under effect of a magnetic field in a non-uniform channels*, Applied Mathematics and Computation **153** (2004), no. 3, 763–777.

[20] Kh. S. Mekheimer, E. F. El Shehawey, and A. M. Elaw, *Peristaltic motion of a particle fluid suspension in a planar channel*, International Journal of Theoretical Physics **37** (1998), no. 11, 2895–2920.

[21] A. M. E. Misery, A. E. Hakeem, A. E. Naby, and A. H. E. Nagar, *Effects of a fluid with variable viscosity and an endoscope on peristaltic motion*, Journal of the Physical Society of Japan **72** (2003), no. 1, 89–93.

[22] M. Mishra and A. Ramachandra Rao, *Peristaltic transport of a Newtonian fluid in an asymmetric channel*, Zeitschrift für Angewandte Mathematik und Physik **54** (2003), no. 3, 532–550.

[23] A. Ogulu and T. M. Abbey, *Simulation of heat transfer on an oscillatory blood flow in an indented porous artery*, to appear in International Communications in Heat and Mass Transfer.

[24] C. Pozrikidis, *A study of peristaltic flow*, Journal of Fluid Mechanics **180** (1987), 515–527.

[25] K. R. Rajagopal, *Mechanics of non-Newtonian fluids*, Recent Developments in Theoretical Fluid Mechanics (Paseky, 1992) (G. P. Gladi and J. Necas, eds.), Pitman Res. Notes Math. Ser., vol. 291, Longman Scientific & Technical, Harlow, 1993, pp. 129–162.

[26] K. K. Raju and R. Devanathan, *Peristaltic motion of a non-Newtonian fluid; Part II. Visco-elastic fluids*, Rheologica Acta **13** (1974), no. 6, 944–948.

[27] A. R. Rao and S. Usha, *Peistaltic transport of two immiscible viscous fluids in a circular tube*, Journal of Fluid Mechanics **298** (1995), 271–285.

[28] H. J. Rath, *Ein Beitrag zur Berechnung einer peristaltischen Strömung in elastischen Leitungen*, Acta Mechanica **31** (1978), no. 1-2, 1–12.

[29] A. H. Shapiro, M. Y. Jaffrin, and S. L. Weinberg, *Peristaltic pumping with long wavelength at low Reynolds number*, Journal of Fluid Mechanics **37** (1969), 799–825.

[30] G. C. Sharma, M. Jain, and A. Kumar, *Performance modeling and analysis of blood flow in elastic arteries*, Mathematical and Computer Modelling **39** (2004), no. 13, 1491–1499.

[31] A. M. Siddiqui, A. Provost, and W. H. Schwarz, *Peristaltic pumping of a second order fluid in a planar channel*, Rheologica Acta **30** (1991), no. 3, 249–262.

[32] A. M. Siddiqui and W. H. Schwarz, *Peristaltic pumping of a third order fluid in a planar channel*, Rheologica Acta **32** (1993), no. 1, 47–56.

[33] ———, *Peristaltic flow of a second order fluid in tubes*, Journal of Non-Newtonian Fluid Mechanics **53** (1994), 257–284.

[34] D. Srinivasacharya, M. Mishra, and A. R. Rao, *Peristaltic pumping of a micropolar fluid in a tube*, Acta Mechanica **161** (2003), no. 3-4, 165–178.

[35] V. P. Srivastava and M. Saxena, *A two-fluid model of non-Newtonian blood flow induced by peristaltic waves*, Rheologica Acta **34** (1995), no. 4, 406–414.

[36] L. M. Srivastava and V. P. Srivastava, *Peristaltic transport of blood: Casson model-II*, Journal of Biomechanics **17** (1984), no. 11, 821–829.

[37] V. K. Sud, G. S. Sephon, and R. K. Misha, *Pumping action on blood flow by a magnetic field*, Bulletin of Mathematical Biology **39** (1977), no. 3, 385–390.

[38] S. Takabataka, K. Ayukawa, and A. Mori, *Peristaltic pumping in circular cylindrical tubes; a numerical study of fluid transport and its efficiency*, Journal of Fluid Mechanics **193** (1988), 267–283.

[39] S. Takabatake and K. Ayukawa, *Numerical study of two-dimensional peristaltic flows*, Journal of Fluid Mechanics **122** (1982), 439–465.

[40] D. K. Wagh and S. D. Wagh, *Blood flow considered as magnetic fluid flow*, Proceeding of Phisological Fluid Dynamics (1992), 311–315.

[41] X. Wu, W. Studer, T. Erb, K. Skarvan, and M. D. Seeberger, *Competence of the internal jugular vein value is damaged by cannulation and catheterization of the internal jugular vein*, Anesthesiology **93** (2000), no. 2, 319–324.

T. Hayat: Department of Mathematics, Quaid-i-Azam University, 45320 Islamabad 44000, Pakistan
Current address: Centre for Differential Equations, Continuum Mechanics, and Applications, School of Computational and Applied Mathematics, University of the Witwatersrand, Johannesburg Private Bag 3, Wits 2050, Johannesburg, South Africa
E-mail address: pensy_t@yahoo.com

E. Momoniat: Centre for Differential Equations, Continuum Mechanics, and Applications, School of Computational and Applied Mathematics, University of the Witwatersrand, Johannesburg Private Bag 3, Wits 2050, Johannesburg, South Africa
E-mail address: ebrahim@cam.wits.ac.za

F. M. Mahomed: Centre for Differential Equations, Continuum Mechanics, and Applications, School of Computational and Applied Mathematics, University of the Witwatersrand, Johannesburg Private Bag 3, Wits 2050, Johannesburg, South Africa
E-mail address: fmahomed@cam.wits.ac.za